ANALYSIS OF CONTROL AND FLIGHT CONFIGURATION REQUIREMENTS FOR MOUNTING PARAMETERS CALIBRATION OF GPS/INS-ASSISTED PHOTOGRAMMETRIC SYSTEMS

A. Habib [a] *, A. P. Kersting [a]

[a] Department of Geomatics Engineering, University of Calgary, Canada, (ahabib, ana.kersting)@ucalgary.ca

Commission I, WG I/5

KEY WORDS: direct sensor orientation, mounting parameters, system calibration

ABSTRACT:

The availability of high accuracy position and orientation information obtained from the integration of GPS and inertial systems allows the direct determination of the image orientation parameters without the need for ground control points. Although several advantages are offered by the direct sensor orientation, precaution should be taken when dealing with multi-sensor systems. In GPS/INS-assisted photogrammetric systems, besides the camera calibration, the geometric relationship between the sensors (mounting parameters) must be known as well. More specifically, the lever-arm offset between the sensors, as well as the misalignment (boresight angles) between the IMU body frame and the photogrammetric camera should be determined. The offsets are usually measured using traditional surveying techniques, while approximate values for the boresight angles are known from the mechanical alignment. Since these initial mounting parameters might be biased, they should be refined through an in-flight calibration. The objective of this paper is to investigate the aspects involved in the design and implementation of an in-flight mounting parameters calibration, as they relate to control and flight configuration requirements. The paper starts with a brief discussion of the concept and prerequisites of GPS/INS-assisted photogrammetric triangulation procedure. Then, a mathematical analysis of the GPS/INS-assisted camera point-positioning equation, leading to the determination of the flight configuration and the control requirements for mounting parameters estimation, is performed. The presented analysis is evaluated through experimental results using simulated and real datasets.

1. INTRODUCTION

Due to fast technological advances, currently most of the airborne mapping systems consists of multi-sensor systems, typically encompassing a GPS/INS and one or two imaging sensors. Traditionally, image-based topographic mapping has been performed using a single sensor, more specifically a large format analogue camera, and the object space reconstruction obtained through an indirect georeferencing procedure, where the image georeferencing parameters and the coordinates of the ground points are determined in a bundle adjustment procedure using corresponding tie points between images and ground control points. Point positioning derived through a traditional indirect georeferencing approach is illustrated in Figure 1. As demonstrated in this figure, the position of an object point $\vec{X}_G$ can be expressed by the summation of two vectors: $\vec{X}_o$ and $\vec{r}$ after applying the rotation $R_c^G{}_{(\omega,\phi,\kappa)}$ and the scale factor λ as presented in Equation 1. In this equation, $\vec{X}_o$ represents the vector from the origin of the ground coordinate system to the camera perspective centre and $R_c^G{}_{(\omega,\phi,\kappa)}$ represents the rotation matrix relating the ground and image coordinate systems. These terms ($\vec{X}_o$ and $R_c^G{}_{(\omega,\phi,\kappa)}$) are the exterior orientation parameters (EOP) of the exposure station, which are determined in the bundle adjustment procedure together with the ground coordinates of the tie points. The term $\vec{r}$ represents the vector from the perspective centre to the image point $(x - x_p - dist_x, y - y_p - dist_y, -c)$ with respect to the image coordinate system. The magnitude of the vector $\vec{r}$, after applying the scale factor λ, corresponds to the distance from the camera perspective centre to the object point. The scale factor λ can be determined from overlapping imagery in the bundle adjustment procedure. The terms (x,y) represent the image coordinates while $(x_p, y_p, c, dist_x, dist_y)$ are the principal point coordinates, the principal distance and the distortions, respectively, which are determined in the camera calibration procedure. The distortions are determined with the help of a distortion model, which is the mathematical representation of the corrections that compensate for various deviations from the assumed collinearity condition. There exist several variations of distortion models that can be used to model inherent distortions such as the Brown-Conrady model (Brown, 1966; Brown, 1971), the USGS Simultaneous Multi-frame Analytical Calibration (SMAC) model (USGS, 2008), and the Orthogonal polynomials model (Ebner, 1976; Grün, 1978). As can be observed in Equation 1, in a traditional indirect georeferencing procedure the photogrammetric system calibration involves only the camera calibration parameters. Experiments have shown that, even for erroneous camera calibration parameters, accurate object space reconstruction might be still obtained (Cramer et. al., 2000; Habib and Shenk, 2001). Due to correlations among the IOP and EOP, uncorrected systematic effects are absorbed by the estimated orientation parameters so that the bundles are optimally fitted to the given control points and a consistent object space reconstruction is still guaranteed.

* Corresponding author.

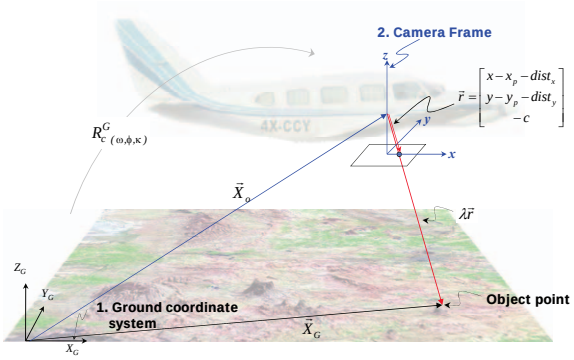

Figure 1. Coordinate systems and involved quantities in the point positioning equation based on indirect georeferencing procedure.

$$\vec{X}_G = \vec{X}_o + \lambda R^G_{c\,(\omega,\phi,\kappa)} \vec{v} = \vec{X}_o + \lambda R^G_{c\,(\omega,\phi,\kappa)} \begin{bmatrix} x - x_p - dist_x \\ y - y_p - dist_y \\ -c \end{bmatrix} \quad (1)$$

The availability of high accuracy position and orientation information obtained from GPS/INS integration process has made it possible to perform direct image orientation without the need for ground control points. The object space reconstruction through direct sensor orientation is illustrated in Figure 2. In the direct sensor orientation, as presented in Equation 2, the position of the object point, $\vec{X}_G$, is derived through the summation of three vectors ($\vec{X}_o$, $\vec{P}_G$, and $\vec{r}$) after applying the appropriate rotations: $R^G_{b\,(yaw,\,pitch,\,roll)}$ and $R^b_{c\,(\Delta\omega,\Delta\phi,\Delta\kappa)}$, and scale factor λ. In this equation, $\vec{X}_o$ is the vector from the origin of the ground coordinate system to the origin of the IMU coordinate system. This vector is derived from the GPS/INS integration procedure while considering the lever-arm offset between the phase centre of the GPS antenna and the IMU body frame. The term $\vec{P}_G$ (lever-arm offset vector) is the offset between the camera perspective centre and IMU coordinate systems (defined relative to the camera coordinate system), while $R^G_{b\,(yaw,\,pitch,\,roll)}$ stands for the rotation matrix relating the ground and IMU coordinate systems (derived through the GPS/INS integration process) and $R^b_{c\,(\Delta\omega,\Delta\phi,\Delta\kappa)}$ represents the rotation matrix relating the IMU and camera frame coordinate systems (defined by the boresight angles). The boresight angles and lever-arm offset are determined in the system mounting parameter calibration procedure. In contrast to indirect georeferencing, where only the camera calibration is needed, direct sensor orientation also involves the system mounting parameters calibration. Moreover, camera calibration plays a more important role in the direct than in the indirect sensor orientation. This is mainly due to the fact that direct sensor orientation is an extrapolation procedure and errors are directly propagated to the object space (Habib and Shenk, 2001). For instance, errors in the calibration parameters cannot be compensated by the exterior orientation parameters. Therefore, reliable camera and system mounting parameters calibration are essential to obtain accurate object space reconstruction.

$$\vec{X}_G = \vec{X}_{GPS/INS} + R^G_{b\,(yaw,\,pitch,\,roll)} R^b_{c\,(\Delta\omega,\,\Delta\phi,\,\Delta\kappa)} \left(\lambda \begin{bmatrix} x - x_p - dist_x \\ y - y_p - dist_y \\ -c \end{bmatrix} - \vec{P}_G \right) \quad (2)$$

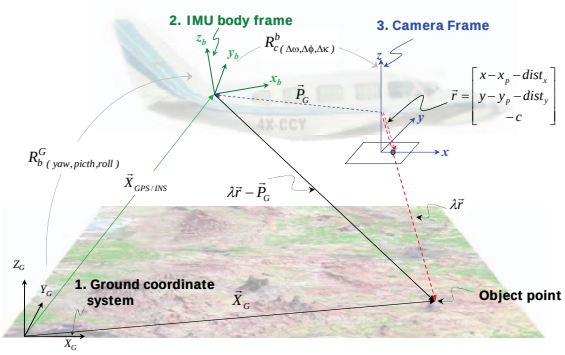

Figure 2. Coordinate systems and involved quantities in the point positioning equation based on GPS/INS-assisted camera system.

Direct sensor orientation can be performed in two different ways: (i) Integrated sensor orientation (ISO) and (ii) Direct georeferencing (Jacobsen, 2004). In the ISO, the GPS/INS derived position and attitude information are used as prior information in the bundle adjustment procedure together with the image coordinates of tie points. This simultaneous adjustment of a number of tie points within a bundle adjustment procedure allows further improvement in the exterior orientation parameters. In the direct georeferencing, on the other hand, the object space coordinates of the image points are obtained from a simple intersection procedure using the GPS/INS derived EOP. The incorporation of the GPS/INS derived position and attitude information in an integrated sensor orientation procedure can be done directly in the collinearity equations, as shown in Equation 2, or it can be done by extending existing bundle adjustment procedures with constraints (i.e., using the model in Equation 1 with the constraints shown in Equations 3 and 4).

$$\vec{X}_{GPS/INS} = \vec{X}_o + R^G_{c\,(\omega,\,\phi,\,\kappa)} \vec{P}_G \quad (3)$$

$$R^G_{b\,(yaw,\,pitch,\,roll)} = R^G_{c\,(\omega,\phi,\kappa)} R^b_{c\,(\Delta\omega,\Delta\phi,\Delta\kappa)}{}^{-1} \quad (4)$$

There exist several factors that might limit the efficient performance of the direct sensor orientation. For instance, the quality of photogrammetric system calibration, the GPS data quality (which is mainly dependent on the distance from the base station, satellite geometry, and continuity of the GPS lock), the type of the IMU system used, and the quality of the GPS/INS integration process. Moreover, the stability of the parameters determined in the calibration procedure is also an issue. Over the last few years extensive investigations on the accuracy performance of GPS/INS-assisted photogrammetric systems have been carried out (e.g., Toth, 1998; Jacobsen, 2000; Cramer et. al., 2000; Wegmann, 2002). The results from the performed investigations, especially the results from the OEEPE test on "Integrated Sensor Orientation" (Heipke et al., 2002), have demonstrated that the accuracy of direct sensor orientation is mainly limited by the quality of the photogrammetric system calibration, which is, as already mentioned, composed by the camera and the system mounting parameters calibration.

Two main approaches can be distinguished in the literature for the estimation of the system mounting parameters: two-step or single-step procedures. In the two-step procedure, the system mounting parameters are estimated by comparing the GPS/INS position and orientation results with the exterior orientation

parameters determined from an independent aerotriangulation (bundle adjustment) solution. Due to its simplicity, i.e., any bundle adjustment software can provide EOP values for the system calibration; the two-step procedure has been extensively used by several authors (e.g., Toth, 1998; Cramer, 1999; Jacobsen, 1999; Skaloud, 1999; Cramer and Stallmann, 2001). However, the two-step approach presents several drawbacks. One of the disadvantages of this method is that correlations among the EOP are ignored and errors in the IOP are absorbed/compensated by the EOP (Cramer and Stallmann, 2002). Moreover, the two-step procedure demands a calibration site with ground control points and a block with very strong geometry to perform the AT (aerial triangulation) procedure. In the single-step procedure, the system mounting parameters are estimated in the bundle adjustment, i.e., through ISO procedure. Therefore, the single step procedure can be done using either of the two available ISO methods. In the first one, existing bundle adjustment procedures are extended with added constraints. More specifically, the traditional mathematical model shown in Equation 1 is extended with the constraints in Equations 3 and 4. This approach has been used by several authors (e.g., Cramer and Stallmann, 2002; Wegmann, 2002, Honkavaara et. al., 2003; Honkavaara, 2004; Yuan, 2008). In the second approach, GPS/INS derived position and attitude information and the system mounting parameters are directly incorporated in the collinearity equations (e.g., Pinto and Forlani, 2002; Habib et al., 2010), i.e., the model in Equation 2 is utilized. Besides less strict flight and control requirements, the single-step is considered a more robust method to handle the dependencies among the EOP and IOP parameters, since the IOP can be refined together with the mounting parameters, if needed. Some authors have empirically investigated flight and control requirements for the single-step in-flight photogrammetric system calibration using real and/or simulated datasets (e.g., Honkavaara, 2003; Pinto and Forlani, 2002; Yuan, 2008). However, a rigorous analysis has not been presented yet and is the focus of this research paper.

The paper starts by introducing a mathematical analysis of the GPS/INS point-positioning equation, leading to the determination of the flight configuration and the control requirements for mounting parameters estimation. Then, the presented analysis is evaluated through experimental results using real datasets. Finally, the paper presents some conclusions and recommendations for future work.

2. IN-FLIGHT SYSTEM MOUNTING PARAMETERS CALIBRATION: FLIGHT AND CONTROL CONFIGURATION REQUIREMENTS

In this section, the optimum flight configuration and the minimum ground control requirement for the estimation of the system mounting parameters is investigated. Such investigation is carried out through mathematical analysis of the GPS/INS-assisted camera point positioning equation (Equation 2).

The following assumptions are considered in the proposed analysis: (i) after the GPS/INS integration, the position refers to the origin of the IMU coordinate system and the attitude refers to the orientation of the IMU body frame, (ii) flight direction is parallel to the positive direction of the X-axis of the IMU coordinate system, (iii) the flight lines follow a straight-line trajectory with constant attitude, and (iv) the camera has relatively small boresight angles (w.r.t. the IMU body frame).

The rationale behind the rigorous analysis, proposed in this research work, to devise the optimum flight configuration requiring minimum control is as follows:

I. Check whether inaccurate/biased mounting parameters would lead to y-parallax between conjugate light rays from directly georeferenced stereo-imagery. In such case, the parameters can be estimated through the elimination/minimization of the y-parallax among conjugate light rays in stereo-imagery. Mounting parameters falling in this category can be estimated using a stereo-image pair without the need for any ground control points.

II. Check whether inaccurate/biased mounting parameters would lead to biases in the derived object points, whose magnitudes and directions depend on the flight configuration. In such a case, one can devise a flight configuration that maximizes the impact of biases in the system mounting parameters on the derived object space. Therefore, using such a configuration, the system mounting parameters can be estimated while reducing the discrepancy among the derived object points from the overlapping imagery (i.e., achieving the best precision of the derived object points). The system mounting parameters falling in this category can be estimated without the need for any ground control points.

III. For the system mounting parameters, which will not introduce y-parallax between conjugate light rays or discrepancies between derived points from overlapping imagery in a given flight configuration, control points will be utilized to derive such parameters. In other words, the mounting parameters falling in this category will be estimated while reducing the discrepancy between the derived object space from the directly georeferenced imagery and the provided control.

In order to investigate whether biases in the system mounting parameters will introduce artificial parallax, we will generate a pair of normalized images from the stereo-pair under consideration. More specifically, the normalized image plane will be defined as being parallel to the xy-plane of the IMU body frame (Figure 3). After rearranging the terms in Equation 2 we can get the forms in Equations 5 and 6. In these equations, the terms $\Delta X, \Delta Y, \Delta Z$ are the components of the lever-arm offset vector $\vec{P}_G$, X_c, Y_c, Z_c are the coordinates of the object point w.r.t. the camera coordinate system shifted to the origin of the IMU coordinate system, and λ the scale factor, while the terms $x_n, y_n, -c_n$ represent the normalized image coordinates and λ_n is the scale factor for a given normalized principal distance.

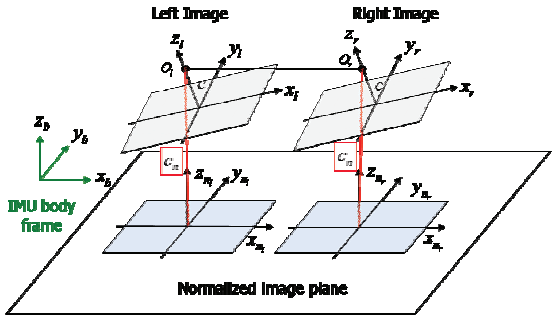

Figure 3. Generated normalized image pair, i.e., the xy-image plane is parallel to the xy-plane of the IMU body frame.

$$R^{G}_{b\,(yaw,\ pitch,\ roll)}{}^{-1}\left[\vec{X}_G - \vec{X}_{GPS/INS}\right] = R^{b}_{c\,(\Delta\omega,\ \Delta\phi,\ \Delta\kappa)}\left(\lambda\begin{bmatrix} x - x_p - dist_x \\ y - y_p - dist_y \\ -c \end{bmatrix} - \begin{bmatrix} \Delta X \\ \Delta Y \\ \Delta Z \end{bmatrix}\right) =$$

$$= R^{b}_{c\,(\Delta\omega,\ \Delta\phi,\ \Delta\kappa)}\begin{bmatrix} X_c \\ Y_c \\ Z_c \end{bmatrix} = \begin{bmatrix} 1 & -\Delta\kappa & \Delta\phi \\ \Delta\kappa & 1 & -\Delta\omega \\ -\Delta\phi & \Delta\omega & 1 \end{bmatrix}\begin{bmatrix} X_c \\ Y_c \\ Z_c \end{bmatrix} \quad (5)$$

$$\begin{bmatrix} \lambda_n x_n \\ \lambda_n y_n \\ -\lambda_n c_n \end{bmatrix} = \begin{bmatrix} X_c - Y_c\Delta\kappa + Z_c\Delta\phi \\ X_c\Delta\kappa + Y_c - Z_c\Delta\omega \\ -X_c\Delta\phi + Y_c\Delta\omega + Z_c \end{bmatrix} \quad (6)$$

To analyze the impact of the biases in the mounting parameters in the normalized image plane, we will differentiate Equations 7.a and 7.b (obtained by dividing the first two rows in Equation 6 by the third one) with respect to the mounting parameters. The outcome of such analysis, after ignoring higher order terms, corresponds to the displacements (δx_n , δy_n) in the normalized image coordinates caused by each of the mounting parameters biases, presented in Table 1. Based on these derived displacements, it is possible to verify whether or not these displacements will introduce artificial y-parallax. One can note that biases in the $\Delta\phi$ (boresight pitch angle) and $\Delta\kappa$ (boresight yaw angle) will introduce artificial y-parallax. Such finding reveals the possibility of estimating biases in the boresight pitch and yaw angles using a control-free stereo pair.

$$x_n = -c_n \frac{X_c - Y_c\Delta\kappa + Z_c\Delta\phi}{-X_c\Delta\varphi + Y_c\Delta\omega + Z_c} \quad (7.a)$$

$$y_n = -c_n \frac{X_c\Delta\kappa + Y_c - Z_c\Delta\omega}{-X_c\Delta\phi + Y_c\Delta\omega + Z_c} \quad (7.b)$$

To evaluate the impact of the mounting parameters biases on the reconstructed object space, one can introduce the displacements caused by each of these biases to the normalized coordinates from the left and right images. Using such coordinates from the left and right normalized images, the biased object space coordinates can be derived.

Table 1. Displacements in the normalized image coordinates caused by each of the mounting parameters biases

	δx_n	δy_n
$\delta\Delta X$	$-\frac{\delta\Delta X}{\lambda_n}$	0
$\delta\Delta Y$	0	$-\frac{\delta\Delta Y}{\lambda_n}$
$\delta\Delta Z$	$-\frac{x_n}{\lambda_n c_n}\delta\Delta Z$	$-\frac{y_n}{\lambda_n c_n}\delta\Delta Z$
$\delta\Delta\omega$	$\frac{x_n y_n}{c_n}\delta\Delta\omega$	$\left(c_n + \frac{y_n^2}{c_n}\right)\delta\Delta\omega$
$\delta\Delta\phi$	$\left(-c_n - \frac{x_n^2}{c_n}\right)\delta\Delta\phi$	$-\frac{x_n y_n}{c_n}\delta\Delta\phi$
$\delta\Delta\kappa$	$-y_n\delta\Delta\kappa$	$x_n\delta\Delta\kappa$

The impact of the biases in the mounting parameters on the derived object space coordinates is as follows:

- The boresight pitch bias will cause a non-linear shift along the flight direction and a smaller non-linear shift in the across flight direction. Note that we will have an artificial parallax in the across flight direction (Y-parallax) in the object space. The boresight pitch bias will also cause a shift in the Z direction with its magnitude varying linearly along the flying direction. All these effects are dependent on the flying height and direction. The planimetric effect along the flight direction and the vertical effect are dependent on the object point coordinates along the flight direction. The planimetric effect across the flight direction, on the other hand, is dependent on the object point coordinates along and across the flight direction.
- The boresight yaw bias will cause a shift along the flying direction with its magnitude varying linearly across the flight direction. This effect is dependent on the flying height and the object point coordinates across the flight direction. The boresight yaw bias will also cause a shift across the flying direction with its magnitude varying linearly along the flight direction. Note that we will have an artificial parallax in the across flight direction (Y-parallax) in the object space. This effect is dependent on the flying height and the object point coordinates along the flight direction. Both effects are independent of the flying direction. This effect is equivalent to a shearing effect in the X and Y directions (the surface will be distorted).
- The boresight roll bias will cause a constant shift across the flight direction and a shift in the Z direction with its magnitude varying linearly across the flying direction (it will tilt the surface in the across flight direction). Both effects are dependent on the flying height and direction. The planimetric effect across the flight direction is independent of the object point coordinates along and across the flight direction. The vertical effect, on the other hand, is dependent on the *y* image coordinate (the image coordinates in the across flight direction).
- The biases in the lever-arm offset will lead to constant shifts in the derived point cloud. The shifts in the XY-directions are dependent on the flying direction. The shift in the Z-direction, on the other hand, is independent of the flying direction. The planimetric and vertical shifts are independent of the flying height and the object point coordinates along and across the flight direction.

Based on the impact of the biases in the mounting parameters on the derived object space listed above, one can devise the optimum flight configuration that maximizes the impact of biases in the mounting parameters. The impact of the pitch and the yaw bias in the object space reveals the possibility of estimating these parameters from a single flight line, or even a single stereo image pair since an artificial Y-parallax is introduced in the object space. However, having opposite flight lines with almost 100% side lap allows for a better estimate of the boresight pitch angle bias, as well as the boresight roll and the planimetric lever-arm offset biases. Having parallel flight lines with the least overlap possible (e.g., 30 – 50%) would allow for a more reliable estimate of the boresight yaw angle. Note that only a vertical bias in the lever-arm offset parameters cannot be detected by observing discrepancies between conjugate surface elements in adjacent flight strips. Such inability is caused by the fact that a vertical bias in the lever-arm offset parameters produces the same effect regardless of the flying direction, flying height, or image point coordinates. Therefore, at least one vertical ground control point would be required to estimate the vertical component of the lever-arm offset vector. Figure 4 illustrates the devised optimum flight and control configuration for the estimation of the system mounting parameters.

3. EXPERIMENTAL RESULTS

In this section, experimental results using simulated and real datasets are presented to test the validity of optimum flight and control configuration for the estimation of the system mounting parameters devised in this research work.

The synthetic data was simulated using the same configuration of the real dataset, which is illustrated in Figure 5. The real dataset utilized in this research work was acquired by a MFDC

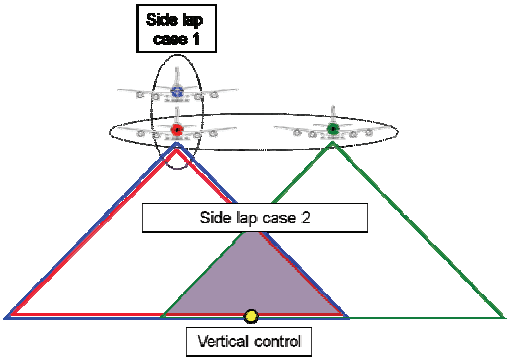

Figure 4. Optimum flight and control configuration for the estimation of the photogrammetric system mounting parameters.

Rollei P-65. This camera has an array dimension of 8984x6732 pixels (53.904x40.392 mm → pixel size = 6μm) and a principal distance of 60 mm. As illustrated in Figure 5, the flight configuration consists of a total of six flight lines acquired in two flight dates, where four flight lines were flown in the E-W direction and two flight lines in the N-S direction, (in opposite directions) with 60% overlap (Figure 5). The flight lines flown in the E-W direction (L1, L2, L3, and L4) were acquired from a flying height of ~550 m (above MSL) and 50% side lap. The flight lines flown in the N-S direction (L5 and L6) were obtained from a flying height of ~1200 m (above MSL) and 100% side lap. A total of 32 images were acquired. It should be noted that the available dataset comply with the optimum configuration discussed in section 2. Also, the GPS/INS derived position and attitude accuracy is ±10 cm and ±10 sec, respectively. In the surveyed area, thirty-seven control points were established (accuracy ±10cm). These control points were used for check point analysis. The camera calibration parameters were determined through an indoor camera calibration technique using the Brown-Conrady distortion model.

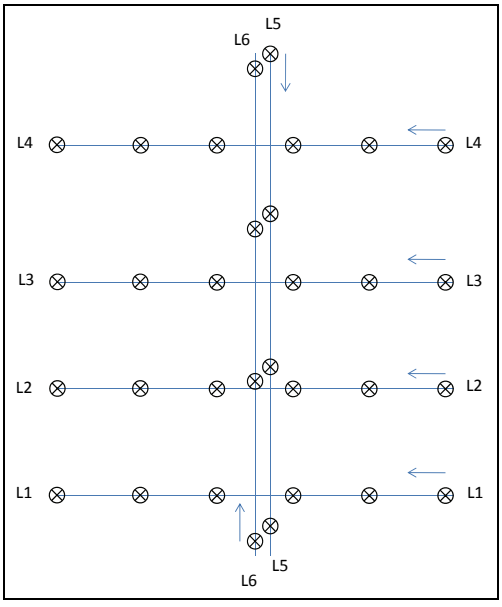

Figure 5. Configuration of the simulated and real datasets.

In the simulated data, the mounting parameters were simulated as 0.50, 0.50, and 1.00m for the lever-arm offset ΔX, ΔY, and, ΔZ, respectively; and 0.50º, 0.50º, and 181º for the boresight angles Δω, Δφ, and Δκ, respectively. The GPS/INS derived position and attitude accuracy was simulated with the same accuracy of the real data, i.e., ±10 cm and ±10 sec, respectively. The accuracy of the simulated vertical control point is ± 10cm. The estimated a-posteriori variance factor and the system mounting parameters as well as the RMSE analysis using the simulated data are reported in Table 2. In this table, we can observe that the estimated system mounting parameters are quite compatible with the introduced ones. Also, the reported accuracy of the estimated mounting parameters and the RMSE values comply with the expected ones based on the accuracy of the navigation data. The presented results confirm the validity of the devised optimum flight and control configuration. In the performed experiments using real data, it could be verified that the given a-priori standard deviation of the available attitude (±10sec) was too optimistic in the adjustment procedure. Therefore, ±100sec was employed instead. Table 3 presents the estimated a-posteriori variance factor, system mounting parameters as well as the RMSE analysis using the devised optimum flight and control requirements. The reported accuracy of the estimated mounting parameters and the RMSE values comply with the ones obtained with the simulated data. It should be noted that the accuracy of the boresight angles was slightly worse than the simulated data due to the degraded quality of the attitude data of the real dataset (100sec).

Table 2. Estimated a-posteriori variance factor, system mounting parameters and RMSE values (ninety-five check points) using simulated data, the devised optimum configuration, and one vertical control point.

$\hat{\sigma}_o^2$ **(mm)²:**	$(0.0030)^2$
***ΔX* (m±m):**	0.5332±0.03
***ΔY* (m±m):**	0.5065±0.03
***ΔZ* (m±m):**	1.1210±0.08
***Δω*(deg±sec):**	0.4994±11.3
***Δφ*(deg±sec):**	0.4976±12.4
***Δκ*(deg±sec):**	181.0036±10.5
***RMS_X* (m):**	0.03
***RMS_Y* (m):**	0.05
***RMS_Z* (m):**	0.17

Table 3. Estimated a-posteriori variance factor, system mounting parameters and RMSE values (thirty-six check points) using real data, the devised optimum configuration, and one vertical control point.

$\hat{\sigma}_o^2$ **(mm)²:**	$(0.0025)^2$
***ΔX* (m±m):**	-0.084±0.05
***ΔY* (m±m):**	-0.124±0.05
***ΔZ* (m±m):**	1.128±0.11
***Δω*(deg±sec):**	-0.1254±18.6
***Δφ*(deg±sec):**	0.8367±18.5
***Δκ*(deg±sec):**	179.5475±22.3
***RMS_X* (m):**	0.09
***RMS_Y* (m):**	0.09
***RMS_Z* (m):**	0.12

4. CONCLUSIONS AND RECOMMENDATIONS FOR FUTURE WORK

In this paper, the optimum flight and control requirements for the in-flight system mounting parameter was established. The paper started with a brief discussion of the concept and

prerequisites of GPS/INS assisted photogrammetric triangulation procedure. Then, a mathematical analysis of the GPS/INS point-positioning equation, leading to the determination of the flight configuration and the control requirements for mounting parameters estimation, was outlined. The validity of the presented analysis was demonstrated through experimental results using simulated and real datasets. Future work will focus on devising an optimum flight configuration for the estimation of the camera IOP, which are susceptible to changes under operational conditions, together with the system mounting parameters in the in-flight system calibration.

ACKNOWLEDGEMENT

This work was supported by the Canadian GEOIDE NCE Network (SII-72) and the National Science and Engineering Council of Canada (Discovery Grant). The authors would like to thank McElhanney Consulting Services Ltd, BC, Canada for providing the real dataset. Also, the authors are indebted to Mr. Dan Tresa, McElhanney Consulting Services Ltd, for the valuable feedback.

REFERENCES

Brown, D., 1966. Decentric distortion of lenses, *Journal of Photogrammetric Engineering & Remote Sensing*. 32 (3): 444-462.

Brown, D., 1971. Close range camera calibration, *Journal of Photogrammetric Engineering & Remote Sensing*. 37 (8): 855-866.

Ebner, H., 1976. Self-calibrating block adjustment, *Congress of the International Society for Photogrammetry*. Invited Paper of Commission III, Helsinki, Finland.

Cramer, M., 1999. Direct geocoding – is aerial triangulation obsolete? In: *Fritsch/Spiller (eds.): Photogrammetric Week 1999*, Wichmann Verlag, Heidelberg, Germany, pp. 59-70.

Cramer, M., D. Stallmann, and N. Haala, 2000. Direct georeferencing using GPS/inertial exterior orientations for photogrammetric applications. *International Archives of Photogrammetry and Remote Sensing*, Vol. XXXIII, Part B3, pp. 198–205.

Cramer, M. and D. Stallmann, 2001. On the use of GPS/inertial exterior orientation parameters in airborne photogrammetry. *ISPRS Workshop "High Resolution Mapping from Space 2001"*, Hannover, Germany, pp. 32-44.

Cramer, M. and D. Stallmann, 2002. System Calibration for Direct Georeferencing. *ISPRS Comm. III Symposium 'Photogrammetric Computer Vision'*, Graz, Austria, 9-13 September 2002.

Grün, A., 1978. Accuracy, reliability and statistics in close-range photogrammetry. *Inter-congress symposium, International Society for Photogrammetry*, Commission V, Stockholm, Sweden.

Habib, A. and T. Schenk, 2001. Accuracy Analysis of Reconstructed Points in Object Space from Direct and Indirect Exterior Orientation Methods. *OEEPE Workshop on Integrated Sensor Orientation*, Institute for Photogrammetry and Engineering Surveying, University of Hannover, 17-18 September, 2001.

Habib, A., A. Kersting, and K. I. Bang, 2010. Comparative Analysis of Different Approaches for the Incorporation of Position and Orientation Information in Integrated Sensor Orientation Procedures. In: *Proceedings of Canadian Geomatics Conference 2010 and ISPRS COM I Symposium*, Calgary, Canada.

Heipke, C., K. Jacobsen, and H.Wegmann, 2002. Analysis of the Results of the OEEPE Test "Integrated Sensor Orientation". *In: Heipke, C., Jacobsen, K., Wegmann, H. (eds.): Integrated Sensor Orientation, Test Report and Workshop Proceedings*, OEEPE Official Publication No. 43, pp. 31-49.

Honkavara, E., R. Ilves, and J. Jaakkola, 2003. Practical results of GPS/IMU camera system calibration. *International Workshop, Theory, Technology and Realities of inertial/GPS Sensor Orientation*, ISPRS WG I/5, Castelldefels, Spain, on CD-ROM, 10 pages.

Honkavaara, E., 2003. Calibration Field Structures for GPS/IMU/Camera-system Calibration. *The Photogrammetric Journal of Finland*, 18(2): 3-15.

Honkavaara, E., 2004. In-Flight Camera Calibration for Direct Georeferencing. *International Archives of Photogrammetry, Remote Sensing and Spatial Information Sciences*, Vol XXXV, Part 1, pp. 166-171.

Jakobsen, K., 1999. Determination of Image Orientation Supported by IMU and GPS. In: *Joint Workshop of ISPRS Working Groups I/1, I/3 and IV/4 – Sensors and Mapping from Space*, Hannover.

Jakobsen, K., 2000. Combined Bundle Block Adjustment versus Direct Sensor Orientation. *ASPRS Annual Convention 2000*, Washington.

Jacobsen, K., 2004. Direct/ Integrated Sensor Orientation – Pros and Cons. *The International Archives of Photogrammetry and Remote Sensing,* Vol. XXXV, Part B3, pp. 829-835.

Pinto, L. and G. Forlani, 2002. A single step calibration procedure for IMU/GPS in aerial photogrammetry. In: *International Archives of Photogrammetry and Remote Sensing*, Vol. XXXIV, Part B3, pp. 210-213.

Skaloud, J., 1999. Optimizing Georeferencing of Airborne Survey Systems by INS/DGPS. Phd Dissertation, Department of Geomatics Engineering, University of Calgary.

Toth, C. K., 1998. Direct Platform orientation of multi-sensor data acquisition systems. *International Archives of Photogrammetry and Remote Sensing*, Vol. XXXII, Part 4, pp. 629-634.

Yuan, X., 2008. A novel method of systematic error compensation for a position and orientation system. *Progress in Nature Science*, 18(8): 953–963.

Wegmann H., 2002. Image Orientation by Combined (A)AT with GPS and IMU. *ISPRS Com. I, Midterm Symposium, Integrated Remote Sensing at the Global, Regional, and Local Scale*, Denver, U.S.A., 10-15 November 2002.

USGS, 2008. Procedure for compensation of aerial camera lens distortion as computed by the simultaneous multiframe analytical calibration (SMAC) systems. http://calval.cr.usgs.gov/ osl/smaccompen.pdf (accessed 9 Dec. 2009).